

Manuscript version: Author's Accepted Manuscript

The version presented in WRAP is the author's accepted manuscript and may differ from the published version or Version of Record.

Persistent WRAP URL:

<http://wrap.warwick.ac.uk/110553>

How to cite:

Please refer to published version for the most recent bibliographic citation information. If a published version is known of, the repository item page linked to above, will contain details on accessing it.

Copyright and reuse:

The Warwick Research Archive Portal (WRAP) makes this work by researchers of the University of Warwick available open access under the following conditions.

© [2018], Elsevier. Licensed under the Creative Commons Attribution-NonCommercial-NoDerivatives 4.0 International <http://creativecommons.org/licenses/by-nc-nd/4.0/>.



Publisher's statement:

Please refer to the repository item page, publisher's statement section, for further information.

For more information, please contact the WRAP Team at: wrap@warwick.ac.uk.

Accepted Manuscript

Title: Investigation of response of high-bandwidth MOX sensors to gas plumes for application on a mobile robot in hazardous environments

Authors: Timothy A. Vincent, Yuxin Xing, Marina Cole, Julian W. Gardner



PII: S0925-4005(18)31563-6
DOI: <https://doi.org/10.1016/j.snb.2018.08.125>
Reference: SNB 25273

To appear in: *Sensors and Actuators B*

Received date: 15-3-2018
Revised date: 23-8-2018
Accepted date: 24-8-2018

Please cite this article as: Vincent TA, Xing Y, Cole M, Gardner JW, Investigation of response of high-bandwidth MOX sensors to gas plumes for application on a mobile robot in hazardous environments, *Sensors and amp; Actuators: B. Chemical* (2018), <https://doi.org/10.1016/j.snb.2018.08.125>

This is a PDF file of an unedited manuscript that has been accepted for publication. As a service to our customers we are providing this early version of the manuscript. The manuscript will undergo copyediting, typesetting, and review of the resulting proof before it is published in its final form. Please note that during the production process errors may be discovered which could affect the content, and all legal disclaimers that apply to the journal pertain.

Investigation of response of high-bandwidth MOX sensors to gas plumes for application on a mobile robot in hazardous environments

Timothy A. Vincent*, Yuxin Xing, Marina Cole, Julian W. Gardner

School of Engineering, University of Warwick, Coventry, UK.

*Corresponding author, t.a.vincent@warwick.ac.uk, +44 (0) 2476 573388.

Timothy Vincent
School of Engineering
University of Warwick
Coventry
CV4 7AL
UK

Highlights

- Custom sensor module developed for use in harsh environments by rescue personnel
- High-bandwidth MOX sensors evaluated to plumes of VOCs inside a wind tunnel
- PdPt SnO₂, WO₃ and NiO coated MOX sensors produce fast responses to low ppm plumes
- Pulse broadening of VOC plumes observed and mapped inside tunnel
- Performance verified in real world, unit is ready for use in hazardous environments

Abstract

A custom sensor module has been developed comprising high-bandwidth metal oxide (MOX), low-cost non-dispersive infra-red (NDIR) and miniature solidly mounted resonator (SMR) acoustic sensors for use on a mobile exploration robot. The module has been tested in a wind tunnel in order to evaluate the performance of three MOX sensors (with coatings of PdPt SnO₂, WO₃ and NiO) to plumes of 2-propanol (concentration < 2.5 ppm). The formation of the VOC (volatile organic compound) plumes was verified through mapping of sensor responses across a grid of 9 positions in the wind tunnel. Fluctuating sensor responses were observed ($\pm 5\%$), demonstrating variation of VOC concentration within the gas plumes. Higher sensor responses were demonstrated with the n-type SnO₂ and WO₃ based devices (80% and 40% change relative to baseline, respectively) compared to the p-type NiO device (10%). Short plumes of VOC demonstrated the effect of gas pulse broadening, where longer duration responses (10% greater) were observed at locations further from the VOC source (~ 0.4 m distance variation tested). Finally, the module was tested in a real-world environment,

where plumes of VOC were observed using the MOX sensors and verified using a commercial PID (Photoionization Detector).

Keywords

MOX gas sensors, plumes, wind tunnel, robotics.

1. Introduction

Firefighting is regarded as one of the most hazardous occupations, with workers regularly exposed to dangerous environments, whether tackling fires or responding to other rescue incidents. Mobile exploration robots offer a safer means of investigating disaster zones, allowing human operators to remotely observe an area without endangering the lives of personnel.

We present the development of a high-bandwidth sensor module (electronic nose), for installation on a mobile robot, as shown in Fig. 1, capable of detecting plumes of VOCs. Plume tracking is of currently a topic of great interest in the field air quality monitoring, where there is great concern of chemicals contributing to air pollution [1-3]. It has been reported that the spatiotemporal nature of chemical plumes challenges the use of gas sensors that rely on capturing precise samples of a gas [4]. Semiconductor sensors are often used for plume tracking, although the slow response times of current MOX devices limits the speed at which the robot can travel.

The VOC sensors inside the module aim to detect the types of gases which present a hazard to rescue teams (e.g. those which can be categorised as either explosive or toxic gases). Target VOCs and gases are carbon monoxide (CO), nitrogen dioxide (NO₂) and hydrocarbons. The end purpose of the sensor module is to mark the locations of such gases and VOCs on a 2-D map (along with other hazards, such as high temperature regions), obtained from a fusion of the data gathered from the mapping sensors. In this preliminary study, this mapping principle has been proven by studying the response of three MOX sensors (with coatings of PdPt SnO₂, WO₃ and NiO) to plumes of 2-propanol with concentrations of less than 2.5 ppm). A wind tunnel is used to simulate the often turbulent and unpredictable air flows often found in disaster environments. The findings from this work will help develop an algorithm used

to track VOC plumes in a real-world scenario, where the sensor module can be mounted on a mobile robot.

This study will contribute to our overall goal of going beyond the current gold standard exploration robots by providing hazard related data to the end users in an easy-to-read format that can help inform decisions and allow rescue teams to respond accordingly.

1.1. Motivation

In the USA, it was reported that out of a workforce of 1.1 million firefighters, eighty thousand injuries are sustained per year [5,6]. Frequent exposure to the polluted environments found in many rescue operations puts firefighters at a greater risk of contracting health complications, such as various cancers (e.g. melanoma, head and neck), coronary heart disease and long-term respiratory diseases [7-9]. The nature of the rescue services' work necessitates fast responses and decisions, which is often based on limited information obtained from emergency evacuation plans.

Mobile reconnaissance robots can significantly reduce the risk to human lives, where rescue teams can explore a hazardous area remotely. The current generation of rescue robots have limited capabilities, and are not usually equipped to identify or map locations of hazards. These robots are typically only able to send visual images and limited environmental data back to the user, and are fitted with basic equipment (e.g. thermal cameras, CO₂ sensor and thermal sensors) [10]. The gas sensor module presented in this work is being developed to be installed on a mobile robot (Gustav, Taurob, Austria), together with a number of other sensors, for example LIDAR (Light Detection and Ranging), radar and imaging cameras, in order to address some of limitations of currently available rescue robots.

Sensors designed for use in the application of mobile exploration must be robust and resilient to harsh environments. Typical sensors used in air quality monitors are not housed for such conditions and have no protection from high temperatures, falling debris or pollution damage. In the case of a robot for use by fire and rescue services, exposure to high temperature is one of the greatest challenges.

Inside a building, the temperature can reach 600°C close to the ceiling of a room during the occurrence of a flashover [11]. Temperatures at lower levels (within 1 m of the ground) can reach between 200 and 300°C. Fires in multi-storey car parks are considered difficult to tackle and extremely hazardous, where the structures are poorly ventilated and it is challenging to identify the source of the fire [3].

1.2. Background

Nanostructured metal oxide sensors are widely used for gas detection. In an n-type granulated porous film (e.g. SnO₂), chemisorbed oxygen species create depletion regions on the grain surfaces. As a reducing gas is introduced, the concentration of free electrons on the surface depletion region increases for n-type semiconductors (i.e. causing a decrease in resistivity). The opposite occurs for a p-type semiconductor (e.g. CuO), i.e. an increase in resistivity when the reducing gas is introduced. The characterisation of miniature MOX sensors used in this work on a benchtop gas testing rig has previously been reported [12]. It has previously been demonstrated that the novel coatings applied to the sensors used in the module provide excellent sensitivity and good selectivity compared to many commercial devices [13]. It has also been reported that the WO₃ coating allows NO₂ to be detected in the ppb range, producing stable results over a range of test environments (e.g. low oxygen) [13].

Here, these sensors are characterised in a custom made wind-tunnel, which generates plumes of VOCs mixed with ambient air. Gas mixtures generated on benchtop rigs are precisely controlled, and enable step changes in gas concentrations (and constant laminar flows). Outside of a laboratory environment, and particularly in exposed outdoor situations, gradual changes in gas concentration are expected, as opposed to step changes.

Air pollution from a point source was first modelled using Gaussian distributions [14]. These first models assumed the plume would broadly travel following the wind direction, with the highest odour concentrations in the centre of the plume, exponentially decreasing away from the wind direction. Gaussian models were developed, with additional terms added to account for reflections and different mixing heights. However, Gaussian models cannot include any photochemistry, and do not describe

the plumes accurately over longer distances. Lagrangian or Eulerian models are preferred for these needs, although Gaussian models are still used to describe plumes from point sources over short distances [15].

The tracking of plumes in a wind tunnel using a mobile robot has previously been reported in the literature [16,17]. Our work significantly improves upon these earlier measurements, which were limited in terms of the slow response times of commercial MOX sensors (> 20 s) or the high cost and unsuitability of the commercial detectors (a photoionization detector, costing > €5000). Fast response sensors are required, to allow the robot to move freely and quickly around an environment. Affordable sensors are preferred for use in harsh safety-critical environments, thus units can be replaced quickly and easily, if any damage is sustained.

The tracking of low concentration VOCs plumes is often not reported, due to the need of sensitive detectors and high-bandwidth responses. Mobile robot tracking (using commercial MOX sensors) has previously been reported with plumes of ethanol and 2-propanol, although plumes were formed from a flow rate of 200 SCCM of each compound, in a laboratory environment (static conditions, air flow speed < 0.03 m/s) [18].

Mobile robots have also been reported to be able to track ions, with the formation of plumes possible inside a wind tunnel. In the work by Harvey [19], the difficulties of tracking plumes were stated, including the “patchy” nature of chemical plumes, requiring algorithms to be developed to consider more aspects than simply magnitude of response. We expand upon these previous works and investigate the formation of VOC plumes in a wind tunnel, using custom MOX sensors and low ppm concentrations of VOCs. To the authors’ knowledge, there is limited exploration in the literature into the characterisation of VOC plumes and no reports of novel NiO coated MOX devices used for the application of mobile robot gas sensing.

In this work, the performance of three novel MOX semiconductor sensors (2 coated with n-type materials and 1 with p-type material) is investigated in a laboratory setting to ppm levels of VOCs. The

three devices are coated with tin dioxide (SnO_2), tungsten trioxide (WO_3) and nickel oxide (NiO), respectively, and enable a wide range of VOCs to be detected. An n-type SnO_2 coating was selected to offer high sensitivity to CO (formed during combustion) [20], which is toxic when inhaled, and therefore is a hazard to rescue teams and occupants alike. The SnO_2 was doped with 2% Palladium and 0.4% Platinum (percentage by mass) to offer enhanced stability. An n-type WO_3 coating was chosen as highly sensitive to NO_2 [13], which was identified as both a toxic and potentially explosive gas. It is used in many production processes, and thus is a potential hazard if a disaster occurs in an industrial zone. A new p-type coating (NiO) was developed to detect ammonia, which is highly toxic. Ammonia is used in many cleaning agents, and is likely to be a potential hazard in domestic or industrial disaster areas.

The polymer coatings are deposited on top of miniature (1 mm x 1 mm) low-cost CMOS devices, which operate with low power-consumption (< 10 mW) and fast stabilisation times (< 60 s). The sensors expand beyond the commercial gold standard, to offer improved performance needed for their use on a mobile robot, travelling through a disaster zone. Our MOX coatings enable fast response times (< 10 s), good selectivity, and excellent stability.

A custom designed wind tunnel is used to simulate the plumes of gases experienced when the sensor module is sampling the ambient air in a hazardous environment. The wind tunnel is operated using a fan to generate an artificial wind, which creates an air flow speed similar to the wind experienced when the robot is exploring a remote location. Two methods are implemented to analyse the response of the sensors to low concentrations of VOCs. The first method is based on sampling the headspace collected from a container of VOC (stored in liquid form) and the second method is based on injecting the liquid VOCs directly into the tunnel (via a spray method).

2. Experimental Setup

A custom designed wind tunnel is used to generate plumes of VOCs. Our novel MOX sensors are installed inside a robust enclosure, which uses a pump to sample gas from the environment. The

results from the MOX sensors inside the portable system are presented, which aim to target the typical VOCs found in hazardous environments (e.g. NO₂, CO etc.). To enable safe laboratory testing, the very hazardous VOCs are replaced with compounds that can safely be exposed using a standard fume cupboard (e.g. ethanol, acetone or 2-propanol). From preliminary experiments, 2-propanol was selected, as all three MOX sensors demonstrated a level of sensitivity to this VOC.

2.1. Wind Tunnel

To safely generate plumes of VOCs, a wind tunnel was designed to operate inside a fume cupboard (to extract the plumes from the exhaust of the tunnel). The tunnel, shown in Fig. 2, was constructed from a semi-cylindrical (0.5 m diameter, 0.8 m length) tube of acrylic (volume 0.08 m³). A fan (Sanyo Denki 109E2024MH001), shown fitted in the inlet plate of tunnel, provided the air flow through the tunnel. To reduce the formation of eddies inside the tunnel, a baffle (constructed from a sheet of acrylic with a grid of 30 mm holes) was fitted at the exhaust end of the tunnel.

The base of the tunnel (formed from an acrylic sheet) was divided into 9 sections (3 × 3 grid), as shown in Fig. 3. The concentration of the plumes of VOC generated in the wind tunnel were measured at each of the 9 locations. The sensor module is shown positioned in the wind tunnel at location B2, with the gas inlet facing the VOC source. A Teensy microcontroller (version 3.2, PJRC) was used to control the rotation speed of the fan, via PWM (Pulse Width Modulation), and thus the air flow through the tunnel; wind speeds were verified using a thermal anemometer (405i, Testo). The air flow speed could be varied between 1.3 m/s and 2.3 m/s. The lower speed was used in these measurements, to closely resemble the speed at which the mobile robot can travel (~ 5 km/h).

A model of the wind tunnel was developed in Solidworks Flow Simulation 2016 to analyse the air flow along the cross-section of the tunnel. The turbulence created by the fan was analysed, using a CAD model of the fan and defining a rotation speed of 1200 rpm. The flow trajectories are shown in Fig. 4.

The simulation demonstrates the initial 0.2 m section of the tunnel following the inlet fan consists of a turbulent mixture of air. The injection of the VOC is not represented in this simulation, however the

VOC would not be homogeneously mixed with the ambient air during this initial section of the tunnel. Towards the exhaust of the tunnel, the air flow is stable and reduced to approximately 1.05 m/s, compared to the air flow through the fan (> 2 m/s).

The semi-circular design of the tunnel enables the air to be evenly distributed across the width of the tunnel. Proceeding the initial turbulent air flow (near the inlet fan) the flow trajectories show the air flow velocities are similar (varying from ~ 0.6 to 1.3 m/s) across the width of the tunnel. The simulations did not include the effect of placing the tunnel inside a fume cupboard (which has an extraction fan to vent the air).

2.2. Sensor Module

The sensor module was designed to be installed on a mobile robot for investigating hazardous environments. The module is designed to detect hazardous gases for rescuers, i.e. gases that are toxic if inhaled and gases that are potentially explosive. Table 1 lists the sensors contained in the module and their target gases.

The coatings for the MOX sensors have been developed in-house, and deposited on CMOS based devices provided by AMS Sensors UK Ltd. The coatings are applied via a manual drop coating technique. The devices require annealing at operating temperature for at least 8 hours prior to use. A photograph of a device is shown in Fig. 5, showing the bare device in (a) and the coated sensor in (b). As stated in table 1, in this work, three different sensor coatings are used, PdPt SnO₂, WO₃ and NiO. The sensors are operated at a constant temperature ($\sim 300^\circ\text{C}$) during these measurements, configured using inbuilt CMOS micro hotplates (power consumption < 0.1 W). As MOX sensors typically operate at temperatures above 100°C but below 500°C [13], initial trials were performed with the sensors operated between 100 and 450°C . An operating temperature of 300°C was selected for all the devices (based on the same AMS micro-hotplate) to provide the optimum balance between lifetime (reduced at higher temperatures) and sensitivity (increased at lower temperatures). Faster response times were

also found at higher temperatures, desired for operation in an environment with rapid changes in gas concentration.

Response data from the gas sensors are recorded on either a computer or on the mobile robot (i.e. using the Robot Operating System, Indigo distribution). During these wind tunnel experiments, a National Instruments LabVIEW (2016) interface was used. The sensor module is connected to the data logging interface via a micro-USB connection. A microcontroller (Teensy 3.6, PJRC) is used to convert the analogue sensor data into a digital signal. Data are logged at a rate of 10 Hz (data can be stored on an internal microSD card if required, at a rate of 100 Hz).

To ensure the module is resilient to the harsh conditions experienced in a disaster environment, the internal components are housed in a steel enclosure (100 mm × 100 mm × 100 mm). A photograph of the module and the enclosure are shown in Fig. 6 (including the internal circuitry). A two stack PCB design was chosen, where the sensor components (operating at 3.3 V) are located on the upper board, while the bulky components (e.g. valves, pump and flow sensor) are located on the lower board (operating at 5.0 V).

Three valves are used in the module (M-Series, Gems Sensors), operating at 5 V (power consumption 0.5 W per valve). Two (NC variants) are used to isolate the unit, when high temperature air is sampled (> 75°C) and a single multi-purpose valve (2 to 1) is used to switch between two gas sampling inlets (connected to the unit via PTFE tubing). When the unit is mounted on the robot, one inlet is located at close to ground level (~0.1 m from the floor) and one is located at a physically high position on the robot (~ 1 m above ground level). This allows the unit to sample gases that are of lower and higher density than air. When inside the wind tunnel, the curvature of the tunnel roof prevents the use of a sampling inlet at a constant raised elevation, thus gas is sampled at ~0.1 m above the floor of the tunnel for all measurements.

The steel enclosure protects the internal components from the harsh environment, but it also prevents the sensor module from sampling gas directly (i.e. passive sampling is not possible). A pump

(D250S, Micropumps) is used to draw a sample of air from the environment through the sensor module (maximum flow rate of 360 ml/min). The pump operates at 5 V (power consumption 0.4 W). A section of the sensor chamber is dedicated to filtering the sampled inlet gas, prior to exposing the sensors to the potentially corrosive gas. The filtering section was designed to remove soot particles and other matter from the inlet gas, to prevent damage to the sensing layers.

2.3. Software Interfaces

A software interface was developed to control the speed of the flow in the wind tunnel. During these experiments, to mimic the wind speed experienced by the mobile robot travelling around a location, pulse width modulation (PWM) control was used to reduce the speed of the air inlet fan (from the maximum of 2000 to 1200 rpm). The microcontroller used to adjust the PWM rate was configured to accept serial inputs from a computer and change the speed of the fan accordingly. A LabVIEW interface was written to enable the speed to be adjusted in a user-accessible manner.

Sensor data were acquired using a separate LabVIEW interface with the integrated microcontroller in the sensor module. The interface was designed to display the following data in real-time: MOX sensor response and heater temperature (in terms of voltage for the 3 MOX sensors); NDIR detector response and emitter temperature (raw voltage displayed); sample air temperature ($^{\circ}\text{C}$), pressure (bar) and humidity (% RH) and the flow rate (SCCM) through the unit. The program allowed for the data to be logged to a NI data file (*.tdms) for analysis.

2.4. VOC Experiment Methodology

Two methods of exposing the sensor module to VOCs were used, either using the head-space of a container of liquid VOC or by spraying the VOC directly into the tunnel. For each method, measurements are taken at each of the 9 locations marked in the tunnel (randomised order). For the first method, the VOC source is located close to the fan inlet to the tunnel, as shown in Fig. 3. A sparger is used to propagate the VOC into the headspace of a container. The air and VOC mixture from the headspace of the container is drawn into the wind tunnel via the inlet fan. A compressed air supply

and a mass flow controller are used to control the flow rate through the sparger (set at a continuous rate of 500 SCCM). The VOC liquid is kept at room temperature (21 °C) during the experiments.

The head-space sampling method was used to visualise the plumes of VOC over a period of 5 minutes. A baseline period (1 min) is recorded at each location, before the VOC is injected (the VOC is then injected for 5 min). A baseline period (5 min) is allowed at the end of each experiment to allow the tunnel to be vented. Fluctuations in the sensor outputs during the 5 min injection period demonstrate the occurrence of plumes of gas. The sparger configuration effectively mixes the VOC with the head-space air, which is then sampled via the inlet fan.

The spray method of injecting the VOC was proposed to demonstrate the high-bandwidth nature of the sensor module. The spray is injected into the tunnel at the rate of 2 Hz. Preliminary measurements found each spray injected a mass of 0.12 g (on average) of liquid into the tunnel. Liquid 2-propanol has a density of 780 kg/m³ [21]. Given the static volume of the wind tunnel (0.08 m³) and assuming atmospheric pressure at 21°C, a single spray injects a 1.9 ppm plume of 2-propanol into the tunnel.

For both methods, the unit is placed at the centre of each of the grid squares in the tunnel. The inlet nozzle is pointed towards the end of the tunnel (towards the wall of the tunnel in which the fan is mounted). The unit is manually moved between locations after each test cycle.

3. Results and Discussion

In this section, the stability and repeatability of the sensors are investigated, and then the results from the sparger injection method are presented, followed by the results from the spray injection method. These two methods are separated, as each tests a different aspect of the sensor module (i.e. in terms of response time and the duration of the gas plumes). For comparison purposes, the response from all the MOX sensors is expressed as a positive value, in terms of resistance change (ΔR). Raw measurement data shows the sensors coated with n-type materials (MOX1 and MOX2) respond with a decrease in measured resistance (to the presence of the VOC), while the sensor coated with a p-type material (MOX3) responds with a positive increase in resistance. In this work, the change of resistance

(ΔR) is calculated as the change in resistance compared to the average zero gas value recorded during the experiment. Its sign (+/-) changes with gas type (reducing and oxidising) as well as MOX type (n-type or p-type).

To investigate the repeatability of the sensor module, the sensors were first trialled in three separate experiments over a period of 3 weeks. At each measurement trial the module was placed at positions B2 and then C3. The average response from each sensor was taken to the injection of 2-propanol (introduced using the head-space method). Additionally, the average baseline was taken from each trial. Fig. 7 shows the repeatability of the sensor responses, (a) and (b) for positions B2 and C3, respectively, and baseline variance (c).

The sensors demonstrate excellent repeatability, considering the large variance of the plumes expected in a wind tunnel scenario. MOX1 and MOX2 sensors demonstrate a worst-case repeatability of <5%, across the measurements at the three trials. The sensors are annealed and stabilised prior to being installed in the module, contributing to the high stability recorded in the wind tunnel experiments. Over the measurements shown, baseline drifts of 6.5 % and 2.5 % were recorded for MOX1 and MOX2, respectively. MOX 3 was installed in the unit, using a novel film coating (NiO). The development of this coating has not reached the mature level of the coatings used on the MOX1 and MOX2 devices. As such, a lower level of repeatability was observed and greater level of baseline drift was present.

3.1. Head-space VOC Plume Injection Method

The headspace was sampled from a container of 2-propanol and drawn into the wind tunnel through the inlet fan. The average speed in the wind tunnel across the measurements was 1.25 m/s. As detailed in the experiment methodology, each position inside the tunnel was tested in a random order (3 repetitions). Response data from one repetition are shown in Fig. 8, when the unit was located at position B2.

Sensor response data observed on a gas rig would ideally demonstrate a step response change to the presence of a VOC, with a stable output value after the response time of the sensor is reached. In these wind tunnel experiments, the enlarged plot inset Fig. 8, demonstrates the fluctuating sensor outputs (MOX1 is shown). This variation is caused by the formation of plumes, which cause patches of the VOC inside the wind tunnel. The response of the MOX sensors at different locations inside the wind tunnel is shown in Fig. 9 (mean values across a 60 s period, for three repetitions). Error bars are used to indicate the standard deviation during this period. Approximate timing of 60 s period shown in Fig. 8.

MOX1 demonstrates a greater response to the 2-propanol plumes, compared to the MOX2 and MOX3 devices, and also the highest variability. A colour map is shown in Fig. 10, showing the concentration of the plumes across the length and width of the tunnel recorded from MOX1.

The colour map shows the higher plume concentration is found nearer the source of the VOC. The responses are taken after the module has been exposed to the VOC for a ~180 s period (thus allowing time for mixing and distribution within the tunnel). Lower concentrations were observed in the centre location B2 and C2, which indicate the higher dispersion rate in the centre of the tunnel in the direct air-flow from the fan. The highest concentration is observed at A2, closest to the 2-propanol source. The fluctuations visible in the sensor outputs add complexity to plume tracking algorithms, where the higher concentrations can be observed at further distances from the source.

3.2. Spray Injection Sampling Method

In this method, plumes of 2-propanol were created using a spray injection system. Data were recorded for each of the 9 positions, again in a random order (and 3 repetitions). The average wind speed recorded in the centre of the tunnel was 1.36 m/s across the measurement periods. A set of data for each position consisted of sensor responses recorded over a 4 min period; 1 min allowed for a baseline reading to be taken, the spray was injected into the tunnel (2 sprays, approx. 1 s total period), followed

by a 3 min period to analyse the response of the sensor. The two sprays inject a 2.4 ppm pulse (total) of 2-propanol was injected into the tunnel for each measurement.

The response data from the three MOX sensors for position B2 is presented in Fig. 11, from one repetition (data filtered using a median filter, width 0.5 s). The change in resistance values are expressed as positive values, regardless of the direction of the sensor response. The response data from the three sensors have also been normalised (relative to the baseline resistance of each device) to allow the sensor response performance to be compared.

The baseline resistances of the three MOX sensors were recorded as 2.62 M Ω , 143 k Ω and 565 k Ω , respectively. The SnO₂ coated sensor (MOX1) produces a large response to the gas, demonstrating a 62% decrease in resistance, compared to a 13% decrease and 2% increase for MOX2 and MOX3, respectively. SnO₂ based sensors are commercially used for the detection of alcohol, where the PdPt doped coating on our novel sensor retains the high sensitivity to such compounds, but with the advantages of increased stability and improved long-term performance (over a period of months).

Data were collected from the 9 positions inside the wind tunnel, and the peak change in resistance extracted for each MOX sensor (defined as the median of the three peak resistances recorded). The average change in resistance ΔR are shown in Fig. 12.

Position A2 produces a higher (a factor of ~ 1.5 greater) response, notably for all 3 sensors. This position is located centrally, and nearest to the VOC injection port. Thus it is exposed to a far greater concentration of the VOC. However, the other positions located in the centre of the tunnel (B2 and C2) demonstrate lower responses, compared to the positions in the sides of the tunnel (i.e. B1, B3 and C1, C3, respectively). Also, sensors located furthest from the inlet fan show a higher response to the VOC. This phenomenon can be displayed on a colour map, as shown in Fig. 13 (data taken from MOX 1).

To investigate the sensor responses over the length of the tunnel, the width of the sensor response pulse was taken from each of the MOX sensors. The average value (from 3 repetitions) was taken, with the pulse width defined as the duration of the pulse from 50% value (between baseline and maximum peak response) until the sensor response returns to 50% value (between maximum peak response and final value at the end of the experiment). A summary of the data from all 3 devices is shown in Fig. 14. Normalised resistance is used to express the response of the gas sensors, relative to the initial baseline resistance, to allow the response magnitudes rather than signs to be compared.

The pulse widths in the central positions A2, B2 and C2 are shorter (in the range of 2 to 3 % decrease) compared to the corresponding side positions in the tunnel, demonstrated by all 3 devices. The flow along the centre of the tunnel, directly in front of the fan, is likely to be greater than that observed in the sides of the tunnel, as shown in the simulation Fig. 4. The shorter pulse widths contribute to the lower pulses observed from the central positions. The response times of the MOX sensors are slower than the injection period for the VOC (1 s). In general, longer pulse widths are observed at the end of the tunnel (pulse broadening). Gaussian models do not predict this sensor output, where central locations are expected to yield greater magnitude responses. It is likely an initial high concentration plume (following a Gaussian distribution) disperses from the tunnel in a short period of time (< 1 s, comparing the 0.8 m tunnel length to the average wind speed 1.3 m/s). These effects necessitate further signal processing, when tracking the source of a VOC in a real world environment.

The concentrations of the VOC observed towards the exhaust of the tunnel are greater, regardless of the position widthways. This demonstrates the VOC mixes with the air inside the tunnel (and the air drawn into the tunnel by the fan). The initial injected concentration measured is greater than the surrounding positions (i.e. A2 compared to A1, B2 etc.), as the initial injection of the VOC is concentrated in the volume close to the inlet port.

As the VOC mixes with the air inside the tunnel, there are patches of high and low concentrations, which are not observable using MOX sensors (response time too low for the given size of the wind

tunnel in this work). The gas in the positions closest to the exhaust end of the tunnel contains a well-mixed combination of VOC and air. This consistent, but lower, concentration produces a higher response from the MOX sensors (i.e. the sensors have a similar effect to a low-pass filter, where short but high magnitude peaks in concentration are attenuated).

3.3. Plumes Outside of Wind Tunnel

The response of the sensor module to plumes of 2-propanol was verified in a real-world environment, outside of the laboratory wind tunnel, during a preliminary test prior to testing the module on the mobile robot. A 2-propanol source (sparger configuration) was placed a distance of 0.7 m from the module gas sampling inlet. The module was exposed to the gas plumes for a period of 350 s. The levels of VOC present were also measured using a commercial PID (ppbRAE 3000, RAE Systems). Fig. 15 shows the results from the MOX1 and MOX2 sensors, compared to the commercial device (MOX3 was not available during these measurements).

The high level of variance shown in the sensor outputs (i.e. MOX1 decreases in resistance up to 50% relative to baseline) demonstrate the formation of VOC plumes. During these measurements, the rate of 2-propanol generation and distance to the source were kept constant (no external wind source was used). The plumes are confirmed by the PID output, with a variance recorded from ~ 2 to 15 ppm. These plumes follow a similar unpredictable nature, observed in the wind tunnel testing. ~~When the module is used to localise VOC sources on the mobile robot, data will need to be analysed considering longer periods of time (e.g. >10 s, compared to instantaneous snapshots) to counter the fluctuating nature of the gas plumes.~~ The module is suitable for use on a mobile robot, although the unavoidable fluctuating nature of gas plumes necessitates careful sampling methodology. Instantaneous snapshots of sensor data are not sufficient to create an accurate gas map of an area (nor locate a VOC source). Samples over a longer period (e.g. >10 s) are required to counter the response variability introduced by the fluctuating VOC concentrations found in a gas plume.

4. Conclusions

In this work we investigate the formation of gas plumes in both a custom laboratory wind tunnel (base size 0.8 m length by 0.5 m width) and a real-world environment. In the literature, sensors are usually characterised using data from gas rigs, which produce controlled, step changes in gas mixtures. In the real world, for the application of mobile robot exploration, gas sources (for example containers of liquid VOCs) do not emit steady concentrations, instead plumes are developed, which create regions of high and low concentrations in the environment.

Three novel CMOS based MOX sensors are tested, coated with PdPt doped SnO₂, WO₃ and NiO. Two methods of injecting a VOC source into the wind tunnel were tested; a head-space sampling method creating plumes over a longer period (5 min), and a spray injection method, creating short (1 s), low concentration (< 2.5 ppm) plumes. 2-Propanol was selected as a target VOC for this work as it is safe to use in a laboratory environment and all three sensors demonstrated a response to it. The SnO₂ coated device produced a high response to the head-space VOC plumes (> 80% decrease in resistance compared to baseline) compared to lower responses from the WO₃ and NiO devices (decrease ~ 40% and increase of 10% baseline resistances, respectively). Plumes towards the end of the tunnel furthest from the exhaust were recorded as exhibiting lower sensor responses, but large fluctuations (> ± 5%) in sensor output were visible, due to the formation of the plumes. These variations necessitate further signal processing in VOC source tracking algorithms, where instantaneous observations of gas concentration are not good indicators of proximity to the source.

Short pulses of VOC were created using a spray injection method, which can only be detected using high-bandwidth sensors. Low ppm plumes were detected using all three MOX sensors; the SnO₂ device produced a greater response (~60% decrease in resistance relative to baseline), compared to the WO₃ and NiO devices (~15% decrease and ~5% increase, respectively). Contrary to the head-space sampling results, higher sensor responses were observed furthest from the source, where pulse broadening effected the sensor outputs. The short pulse injected near the entrance to the tunnel broadened and

mixed with the air inside the tunnel, as it travelled the length of the apparatus. The length of the initial pulse (1 s) is shorter than the response time of the MOX sensors (< 10 s), which then act as low-pass filters (high frequency peaks are attenuated). This effect was confirmed by observing the length of the pulses recorded from the sensor output, which had $\sim 10\%$ longer duration near the exhaust of the tunnel. It is likely this effect will be greater in a real-world scenario, with greater distances from the source compared to the wind tunnel length. A preliminary experiment was conducted to test the sensor module outside of the laboratory, in a real-world environment. Plumes of VOC were observed (large fluctuations in sensor response), confirmed using a commercial PID. To meet the main goal of tracking VOC locations in disaster environments, an algorithm must be developed to account for the unpredictable nature of gas plumes. Improvements to sensor response time are currently considered, through inverse filtering or thermal modulation, to aid the detection of short pulses of VOCs. We believe that this work will enable the gas sensor module to be easily integrated on a mobile robot and used by firefighters to map out hazardous environments in disaster situations.

References

- [1] J. Hodgkinson, Q. Shan, R.D. Pride, Detection of a simulated gas leak in a wind tunnel, *Meas. Sci. Technol.* 17 (2006) 1586–1593. doi:10.1088/0957-0233/17/6/041.
- [2] M. Schmuker, V. Bahr, R. Huerta, Exploiting plume structure to decode gas source distance using metal-oxide gas sensors, *Sensors Actuators B Chem.* 235 (2016) 636–646. doi:10.1016/j.snb.2016.05.098.
- [3] X.G. Zhang, Y.C. Guo, C.K. Chan, W.Y. Lin, Numerical simulations on fire spread and smoke movement in an underground car park, *Build. Environ.* 42 (2007) 3466–3475. doi:10.1016/j.buildenv.2006.11.002.
- [4] T.C. Pearce, J. Gu, E. Chanie, Chemical source classification in naturally turbulent plumes, *Anal. Chem.* 79 (2007) 8511–8519. doi:10.1021/ac0710376.
- [5] D.L. Smith, Firefighter Fitness, *Curr. Sports Med. Rep.* 10 (2011) 167–172. doi:10.1249/JSR.0b013e31821a9fec.
- [6] A. Fabio, M. Ta, S. Strotmeyer, W. Li, E. Schmidt, Incident-level risk factors for firefighter injuries at structural fires., *J. Occup. Environ. Med.* 44 (2002) 1059–63.
- [7] C.S. Baxter, C.S. Ross, T. Fabian, J.L. Borgerson, J. Shawon, P.D. Gandhi, et al., Ultrafine Particle Exposure During Fire Suppression—Is It an Important Contributory Factor for Coronary Heart Disease in Firefighters?, *J. Occup. Environ. Med.* 52 (2010) 791–796. doi:10.1097/JOM.0b013e3181ed2c6e.
- [8] D.M. Gaughan, J.M. Cox-Ganser, P.L. Enright, R.M. Castellan, G.R. Wagner, G.R. Hobbs, et al., Acute Upper and Lower Respiratory Effects in Wildland Firefighters, *J. Occup. Environ. Med.* 50 (2008) 1019–1028. doi:10.1097/JOM.0b013e3181754161.

- [9] R.J. Tsai, S.E. Luckhaupt, P. Schumacher, R.D. Cress, D.M. Deapen, G.M. Calvert, Risk of cancer among firefighters in California, 1988-2007, *Am. J. Ind. Med.* 58 (2015) 715–729. doi:10.1002/ajim.22466.
- [10] F. Matsuno, N. Sato, K. Kon, H. Igarashi, T. Kimura, R. Murphy, Utilization of Robot Systems in Disaster Sites of the Great Eastern Japan Earthquake, in: K. Yoshida, S. Tadokoro (Eds.), *F. Serv. Robot. Results 8th Int. Conf.*, Springer Berlin Heidelberg, Berlin, Heidelberg, 2014: pp. 1–17. doi:10.1007/978-3-642-40686-7_1.
- [11] R.J. Crewe, A.A. Stec, R.G. Walker, J.E.A. Shaw, T.R. Hull, J. Rhodes, et al., Experimental results of a residential house fire test on tenability: temperature, smoke, and gas analyses., *J. Forensic Sci.* 59 (2014) 139–54. doi:10.1111/1556-4029.12268.
- [12] J.W. Gardner, G. Wei, T.A. Vincent, K. Volans, P. Tremlett, T. Wotherspoon, et al., A gas sensor system for harsh environment applications, in: *Procedia Eng.*, 2015: pp. 275–278. doi:10.1016/j.proeng.2015.08.608.
- [13] B. Urasinska-Wojcik, T.A. Vincent, M.F. Chowdhury, J.W. Gardner, Ultrasensitive WO₃ gas sensors for NO₂ detection in air and low oxygen environment, *Sensors Actuators, B Chem.* 239 (2017) 1051–1059. doi:10.1016/j.snb.2016.08.080.
- [14] A. Daly, P. Zannetti, *Air Pollution Modelling - An Overview*, in: *Ambient Air Pollut.*, The Arab School for Science and Technology, 2007.
- [15] W.A.H. Asman, Modelling the atmospheric transport and deposition of ammonia and ammonium: an overview with special reference to Denmark, *Atmos. Environ.* 35 (2001) 1969–1983. doi:https://doi.org/10.1016/S1352-2310(00)00548-3.
- [16] J. Fonollosa, I. Rodríguez-Luján, M. Trincavelli, R. Huerta, Dataset from chemical gas sensor array in turbulent wind tunnel, *Data Br.* 3 (2015) 169–174. doi:10.1016/j.dib.2015.02.014.

- [17] D. Martínez, E. Clotet, M. Tresanchez, J. Moreno, J.M. Jiménez-Soto, R. Magrans, et al., First characterization results obtained in a wind tunnel designed for indoor gas source detection, 2015 Int. Conf. Adv. Robot. (2015) 629–634. doi:10.1109/ICAR.2015.7251522.
- [18] V. Hernandez Bennetts, A.J. Lilienthal, P.P. Neumann, M. Trincavelli, Mobile Robots for Localizing Gas Emission Sources on Landfill Sites: Is Bio-Inspiration the Way to Go?, Front. Neuroeng. 4 (2012) 20. doi:10.3389/fneng.2011.00020.
- [19] D.J. Harvey, Tien-Fu Lu, M.A. Keller, Comparing Insect-Inspired Chemical Plume Tracking Algorithms Using a Mobile Robot, IEEE Trans. Robot. 24 (2008) 307–317. doi:10.1109/TRO.2007.912090.
- [20] N. Bârsan, J.R. Stetter, Findlay M., W. Göpel, High-Performance Gas Sensing of CO: Comparative Tests for Semiconducting (SnO₂-Based) and for Amperometric Gas Sensors, Anal. Chem. 71 (1999) 2512–2517. doi:10.1021/ac981246d.
- [21] M. Holtzhauer, Basic Methods for the Biochemical Lab, Springer Berlin Heidelberg, Berlin, Germany, 2006. doi:10.1007/3-540-32786-X.

Brief Biographies



Timothy Vincent is a research fellow at the University of Warwick. His research interests include Breath analysis, MOX gas sensors and microcontroller based systems for portable gas sensing.



Yuxin Xing is a PhD student at the University of Warwick. Her research interests include signal processing of MOX sensor data, NDIR optical sensors and development of sensor systems for harsh environments.



Marina Cole is a reader at the University of Warwick. Her research interests include biosensors, acoustic sensors and high bandwidth sensors.



Julian Gardner is a professor at the University of Warwick and the head of the microsensors and bioelectronics group at the University. His expertise is in the design of MEMS based chemical sensors and signal processing/data analysis of sensor arrays.

Fig. 1 Photograph of the unique gas sensor module mounted on the rear of the tracked mobile robot 'Gustav' (Taurob, Austria).

Fig. 2 Photograph of wind tunnel, showing inlet fan and high-bandwidth sensor module.

Fig. 3 Diagram showing layout of wind tunnel with 9 sections marked inside tunnel. Two methods of exposing sensor module to VOCs are shown, Method 1 head-space sampling and Method 2 spray injection through port in tunnel roof.

Fig. 4 Top view of the flow simulation of the wind tunnel with velocities (m/s) shown along the length of the tunnel. Inlet fan is on left of diagram with exhaust (atmospheric pressure) represented at right-hand end.

Fig. 5 Photograph of the CMOS based MOX sensor (CCS_09C, AMS Sensors UK Ltd), (a) bare device without coating, and (b) with coating applied to sensor surface.

Fig. 6 Photograph of the steel enclosure and sensor module, including internal circuitry with gas sensor PCB and control PCB.

Fig. 7 Repeatability of sensor responses investigated at (a) position B2 and (b) position C3, over a period of weeks. Baseline drift recorded across the trials (c) for the three MOX sensors. When devices are exposed to the VOC, a decrease in measured resistance was observed (negative change) for n-type sensors and an increase observed (positive change) for the p-type device. ΔR readings shown as positive values for both cases.

Fig. 8 MOX sensor response data from one repetition when module was located at position B2 in the wind tunnel. Enlarged view shows plumes of VOC visible in the response of the MOX sensors. When devices are exposed to the 2-propanol, a decrease in measured resistance was observed (negative change) for n-type sensors and an increase observed (positive change) for the p-type device. ΔR readings shown as positive values for both cases.

Fig. 9 Summary of mean sensor responses to plumes of 2-propanol at the 9 positions in the wind tunnel. Error bars show variance of sensor output during exposure to constant VOC concentration. The ΔR values shown are plotted as positive values for both types of MOX sensor. Prior to processing, a negative change is found for n-type sensors and a positive change is found for the p-type device when exposed to 2-propanol.

Fig. 10 Colour map showing decrease in MOX1 sensor resistance as response to VOC plumes, overlaid on top view of tunnel.

Fig. 11 Sensor response data from the SnO₂, WO₃ and NiO sensors to a plume of 2-propanol, sensor module is located at position B2 in the tunnel. The ΔR values shown are plotted as positive values for both the n-type and p-type MOX sensors. Raw data show a negative change is found for n-type sensors and a positive change is found for the p-type device when the VOC is injected.

Fig. 12 Summary of maxima sensor response data from the 9 positions inside the wind tunnel for the 3 MOX sensors. Prior to processing, when the VOC is injected, a negative change is found for n-type sensors and a positive change is found for the p-type device. The ΔR values were plotted as positive values for both types of MOX sensor.

Fig. 13 Colour map showing the decrease in sensor resistance of MOX1 compared to baseline value, overlaid on a top view of the wind tunnel.

Fig. 14 Comparison of width of sensor response pulses over the length of the wind tunnel. Data shown for 3 MOX sensors.

Fig. 15 Sensor response data when module was exposed to ppm levels of 2-propanol in a real-world scenario.

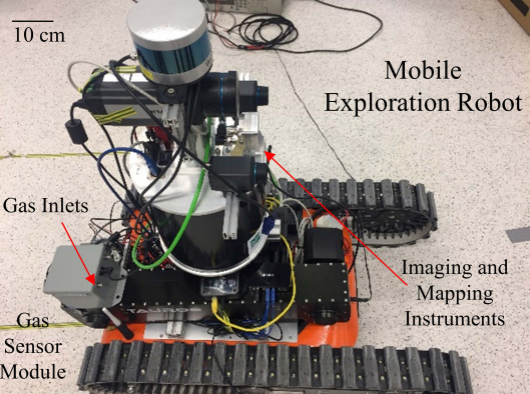
10 cm

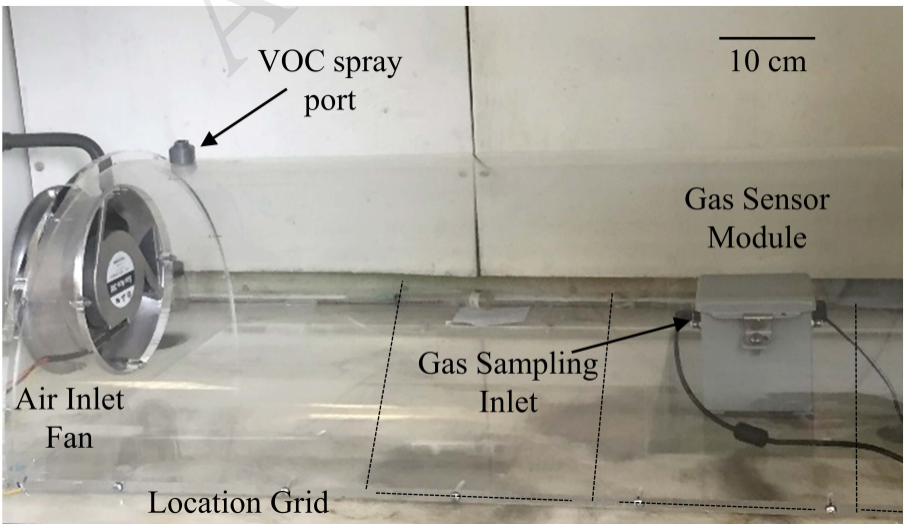
Mobile Exploration Robot

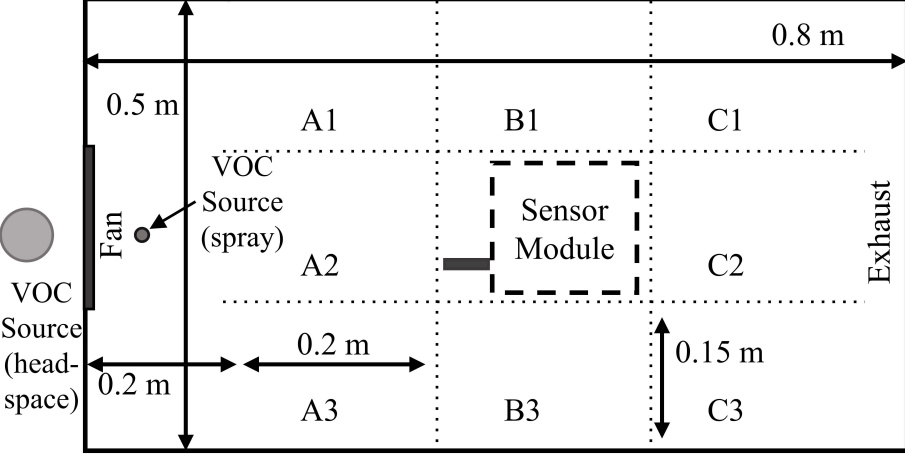
Gas Inlets

Gas
Sensor
Module

Imaging and
Mapping
Instruments

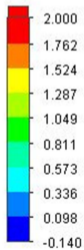
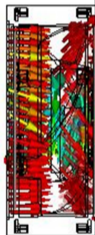






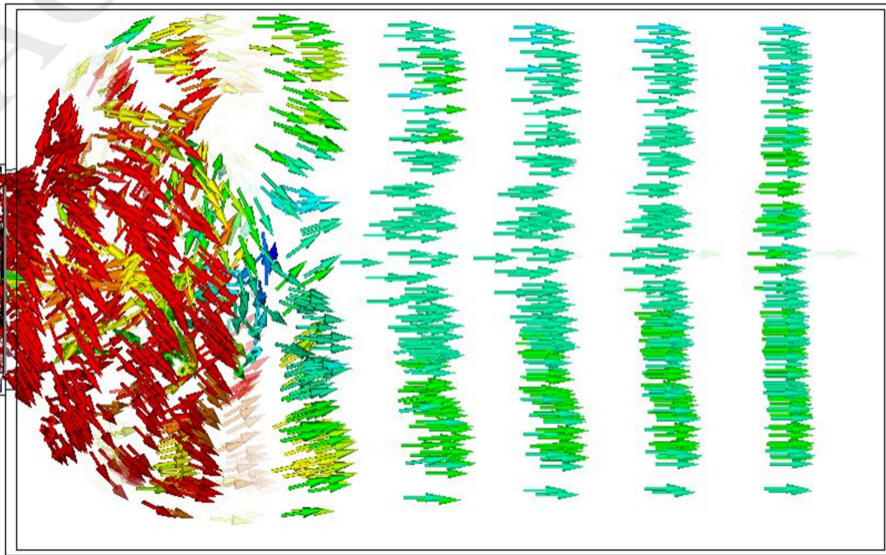
Exhaust

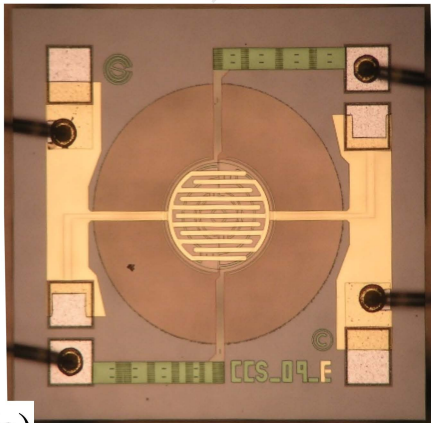
Inlet Fan



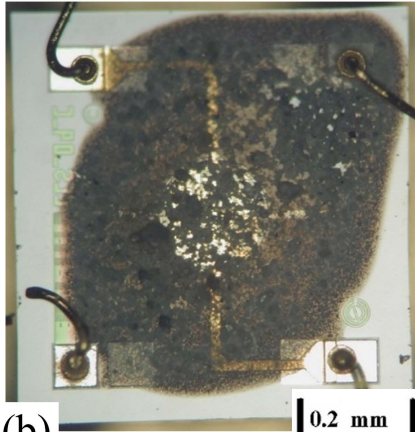
Velocity [m/s]

Flow Trajectories 1





(a)



(b)

Sampling Inlet

Gas Sensor Module

Sensor Chamber

Inlet and
Outlet Tubes

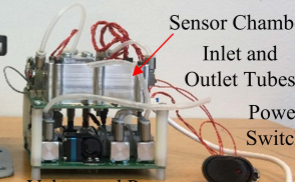
Power
Switch

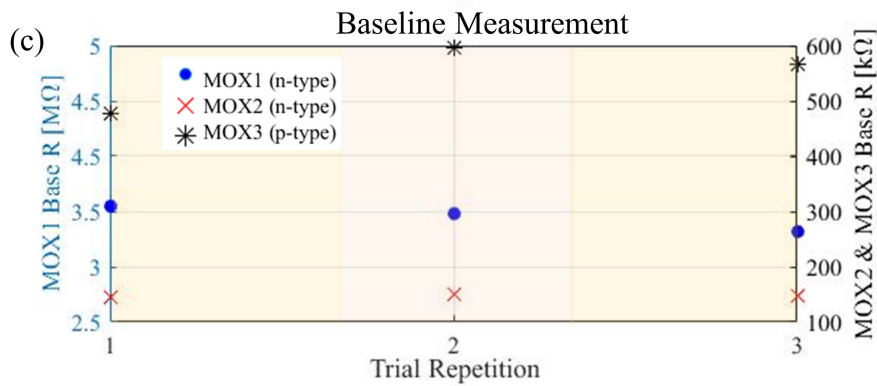
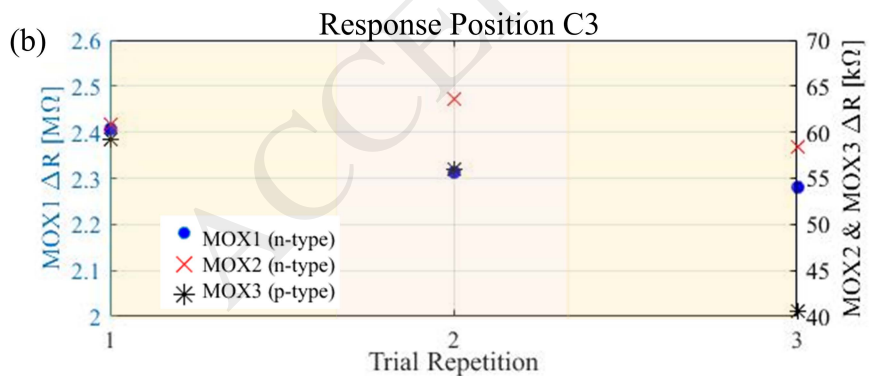
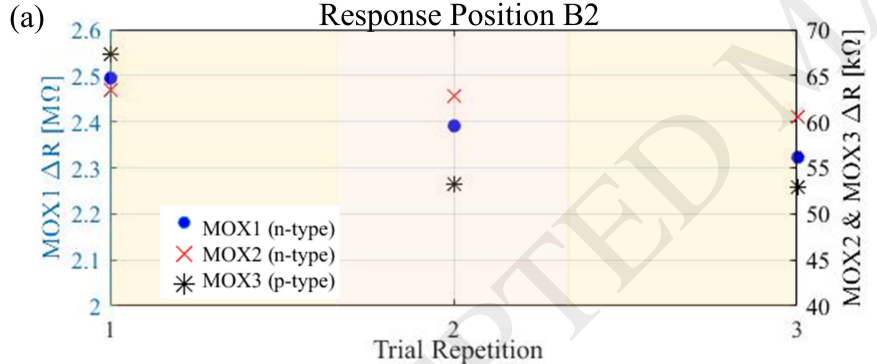
Steel Enclosure

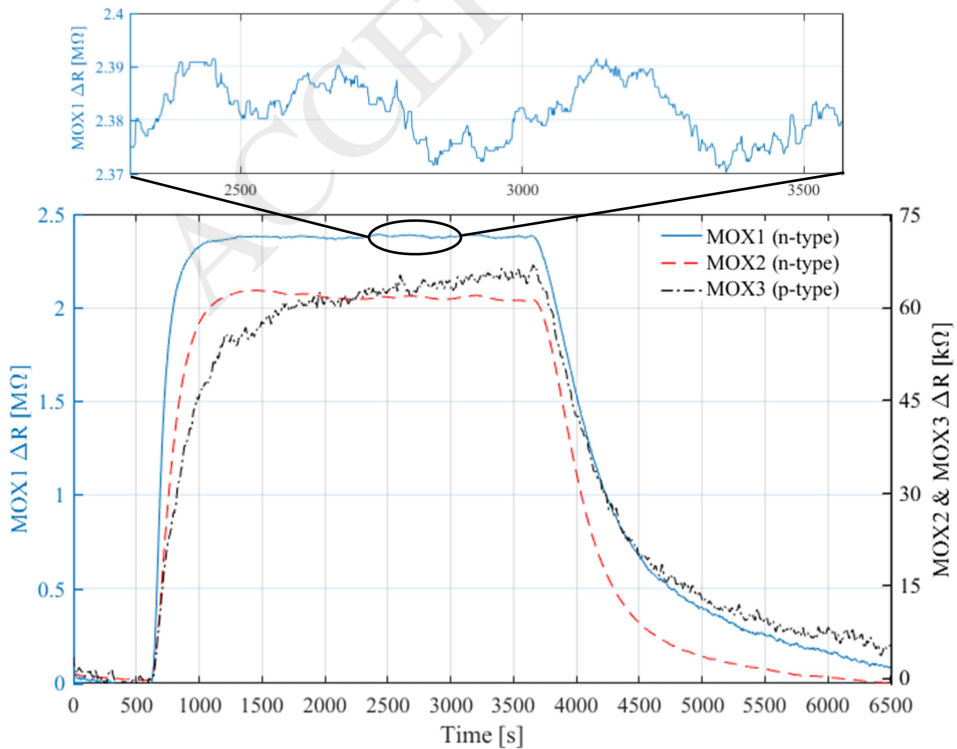
Valves and Pump

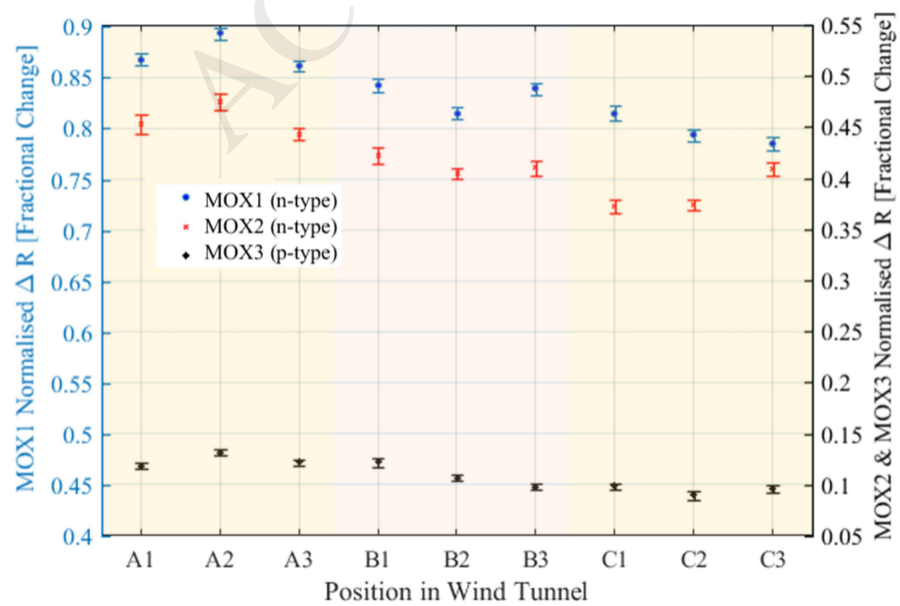
Micro USB
link to Robot

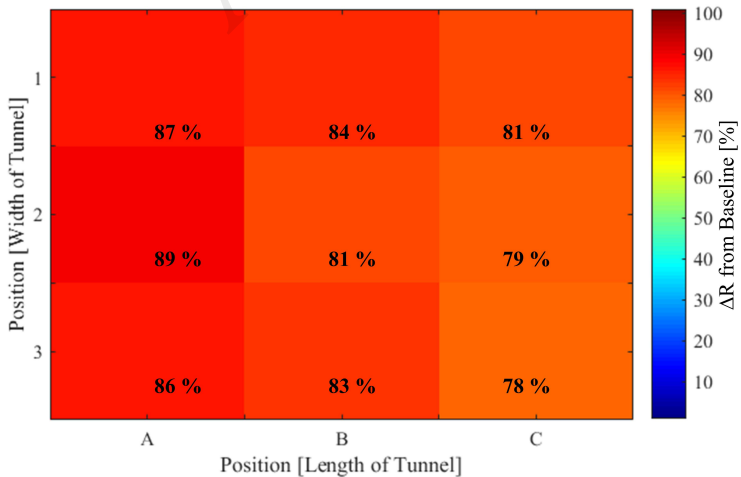
1 cm

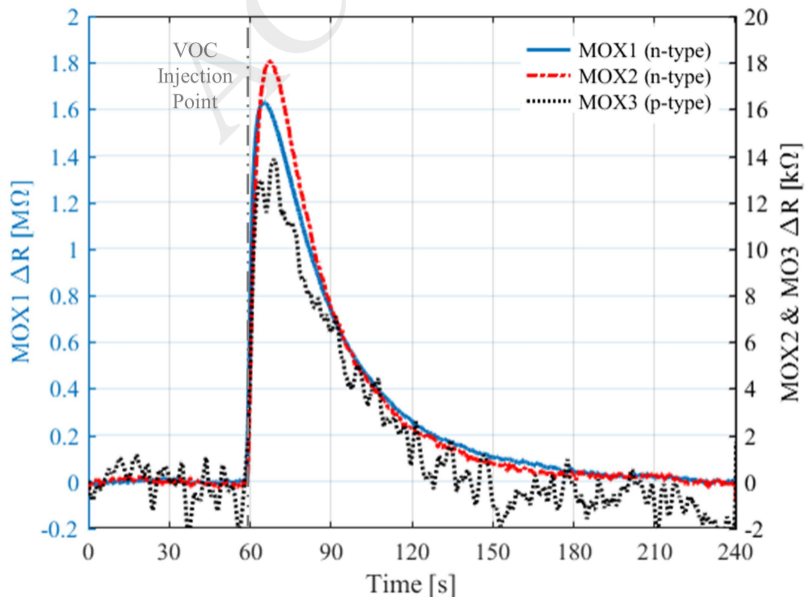


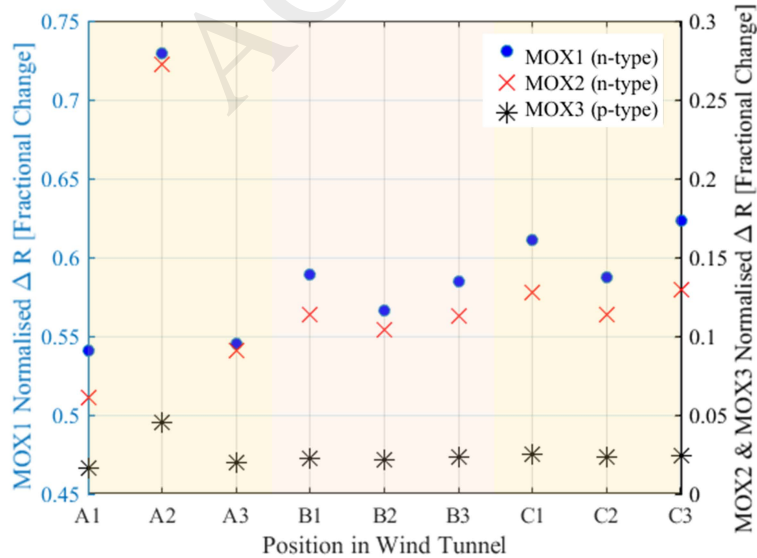


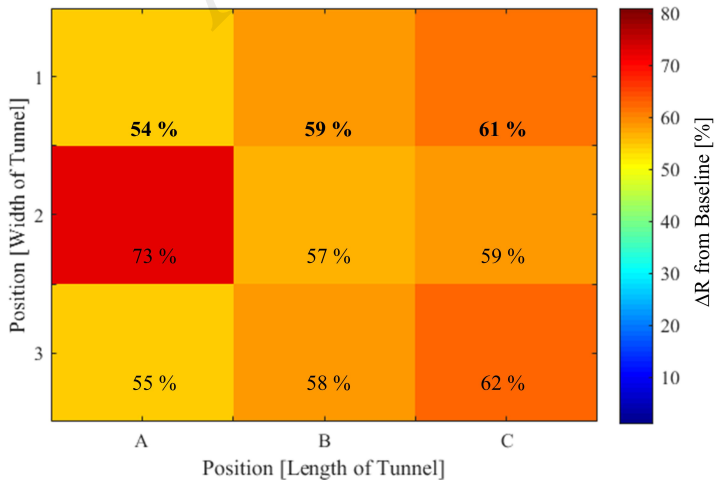


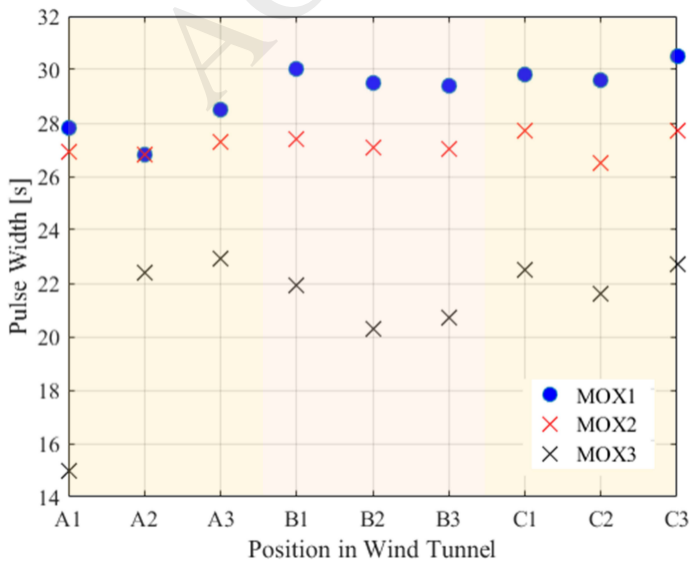












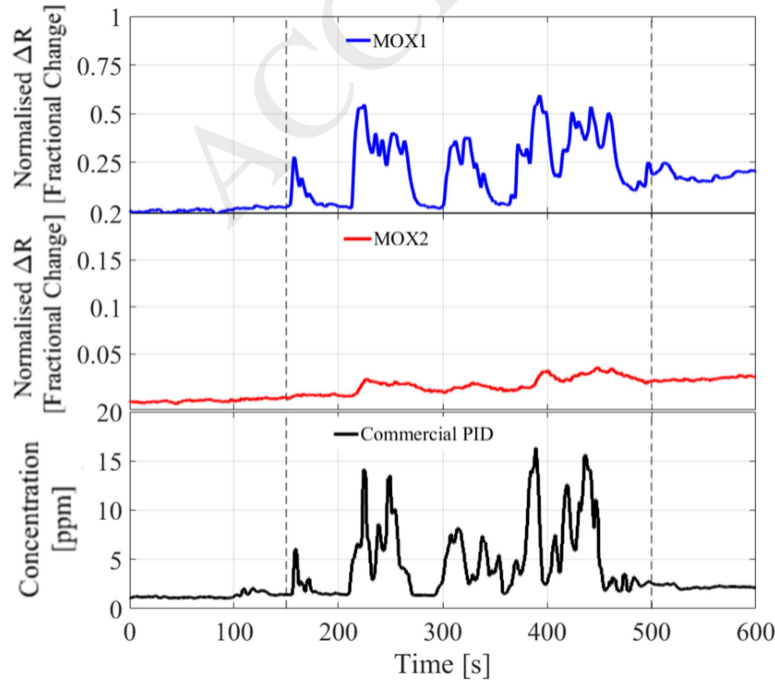


Table 1 – Gas sensor specification for the mobile robot sensor module.

Sensing Principle	Sensor Parameters	Abbreviation	Analyte	Target Detection Range	Supplier
CMOS based MOX	PdPt doped SnO ₂	MOX1	CO	10 – 100 ppm	Internal
	WO ₃	MOX2	NO ₂	ppb level	Internal
	NiO	MOX3	C ₃ H ₆ O	10 – 100 ppm	Internal
CMOS Based SMR	PMMA	SMR	Toluene	ppb level	Internal
CMOS based NDIR optical	Plasmonic Emitter	NDIR	CO ₂	25 ppm	Internal
Temperature Humidity	-	TEMP HUMD	Temperature & Humidity	-40 to 125 °C	Bosch BME280
Particle Sensor	-	PARTICLE	Particle Density	0 to 100 % RH	Isocom H21A3
Flow Sensor	-	FLOW	Flow rate	0 to 750 SCCM	Honeywell HAFBLF0750CAAX5